

## Optical spectra of $\text{Pr}_{2-x}\text{Ce}_x\text{CuO}_{4-\delta}$ crystals: Evolution of in-gap states with electron doping

T. Arima and Y. Tokura

*Department of Physics, University of Tokyo, Tokyo 113, Japan*

S. Uchida

*Superconductivity Research Course, University of Tokyo, Tokyo 113, Japan*

(Received 10 February 1993)

The systematic change of optical conductivity spectra with carrier doping and their anisotropy have been investigated for single crystals of  $\text{Pr}_{2-x}\text{Ce}_x\text{CuO}_{4-\delta}$ ; the crystals were grown by a traveling solvent floating-zone method. The evolution of in-gap states with  $x$  has shown up not only in the growth of midinfrared absorption below the charge-transfer gap but also in higher-lying interband transitions between O  $2p$  and Cu  $4s$  states. Possible roles of the reducing procedure, which is indispensable for producing superconductivity in the electron-doped cuprates, are also discussed in terms of observed changes of the optical spectra.

### I. INTRODUCTION

Insulating  $\text{CuO}_2$ -layered compounds with a nominal Cu valence of +2 can be doped with holes or electrons to act as the charge carriers. By doping the  $\text{CuO}_2$  sheets with an appropriate density of holes or electrons, the compounds can almost always be made to superconduct at high  $T_c$ . In general, the insulating parent compound shows a charge-transfer (CT) gap that is formed between the occupied O  $2p$ -like states and unoccupied Cu  $3d_{x^2-y^2}$ -like states (upper Hubbard band).<sup>1</sup> Naively, doped carriers may show different orbital characteristics in the cases of hole doping and electron doping: that is,  $2p$ -hole character vs  $3d$ -electron character. However, the approximate electron-hole symmetry concerning the occurrence of superconductivity signals that the electronic states near the Fermi level should show common characteristics that are necessary for high- $T_c$  superconductivity. Therefore, to understand the mechanism of high- $T_c$  superconductivity it will be important to see similarities and differences in the changes of electronic structure with hole doping and electron doping. For this purpose, a systematic investigation of doping-induced changes in optical spectra over a wide energy region, i.e., from far-infrared responses due to the charge dynamics near the Fermi level to higher-lying interband transitions reflecting the orbital characters, may be quite useful. Intensive studies have been reported so far on changes of optical spectra with hole-doping in  $\text{La}_{2-x}\text{Sr}_x\text{CuO}_4$  (Ref. 2) and  $\text{YBa}_2\text{Cu}_3\text{O}_{6+y}$ .<sup>3</sup> By contrast, there have been less accumulated optical data for the electron-doped compounds<sup>4</sup> partly due to difficulties in sample preparation.

The  $\text{Pr}_{2-x}\text{Ce}_x\text{CuO}_{4-\delta}$  we have investigated here is an electron-doped cuprate system, which is suitable for the present purpose in the following ways: (1) The compounds can be obtained as single crystals with a sufficient size for spectroscopic studies. (2) The Ce concentration can be well controlled over a wide range including the parent insulator ( $\text{Pr}_2\text{CuO}_4$ ) and superconductor (with

$x=0.15$  and slightly reduced oxygen content). (3) The crystal structure is of the so-called  $T'$ -phase type with crystallographically equivalent  $\text{CuO}_2$  sheets and hence the interpretation is not so complicated as in the case of Y-Ba-Cu-O system with Cu-O chains.<sup>3</sup>

Another important issue to be solved in the case of electron-doped cuprate superconductors is a puzzling role of the reducing procedure which is necessary for producing the superconductivity (at least) in the  $T'$ -phase compounds. Reduced amounts of oxygen ( $\delta$ ) in the superconducting  $T'$ -phase sample,  $\text{Nd}_{2-x}\text{Ce}_x\text{CuO}_{4-\delta}$  ( $x=0.15$ ), have been reported to be as small as 0.01–0.03.<sup>5</sup> The reducing treatment of the compounds with  $x \geq 0.15$  destroys the ordered phase of the Cu spins and causes a transition from the insulator with the magnetic order to the superconducting metal at low temperatures. Nevertheless, changes of lattice constants are too small to be detected by ordinary measurements, in spite of drastic changes of electric and magnetic properties. Optical probes for low-energy electronic states are also expected to yield useful information about an important role of such a reducing procedure.

### II. EXPERIMENT

#### A. Crystal growth by a traveling solvent floating-zone method

The bar-shaped  $\text{Pr}_{2-x}\text{Ce}_x\text{CuO}_{4-\delta}$  single crystals, typically 4 mm in diameter and 3 cm in length, were grown from CuO flux by a traveling solvent floating-zone (TSFZ) method.<sup>6</sup> The crystal growth of the cuprate superconducting systems by the TSFZ method could have many advantages: First, large crystals with thickness across  $\text{CuO}_2$  planes of a few mm can be obtained. Second, the composition of the solid solution system is more homogeneous than by the conventional flux method. Third, contamination from a crucible (Al, Pt, and so on) can be evaded.

The radiation from two halogen lamps was focused

onto a floating solvent zone by double ellipsoidal mirrors. The feeding speed was 0.5–1.0 mm/hour and the crystal was grown in air atmosphere on the (100) surface of the  $\text{Pr}_2\text{CuO}_4$  seed crystal, which beforehand was obtained by a flux method in a Pt crucible. The Ce content of the obtained sample, which was determined from the lattice constant obtained by the x-ray measurement, is almost equal to that of the sintered polycrystalline bar for  $x \leq 0.15$ . An exception is the sample grown from the  $x = 0.20$  polycrystalline bar, in which the lattice constants and superconductivity properties indicated the lower Ce content ( $x \sim 0.17$ ).

The direction of the crystal axis was determined by a Raue photograph. The  $c$  axis of the sample lies across the long axis of the bar, and therefore the area containing the  $c$  axis can be taken to be large enough for measuring anisotropic reflectivity in the far-infrared region. The (001) or (100) surface was cut out from the crystal bar using a diamond cutter.

To control the oxygen content within the samples, some were annealed in flow of oxygen gas at 1000 °C and some in Ar/O<sub>2</sub> gas mixture with partial oxygen pressure of  $1.0 \times 10^{-4}$  atm at 1000 °C. The partial oxygen pressure was monitored by a ZrO<sub>2</sub> sensor. For the undoped sample ( $x = 0$ ), this reduced condition was so strong that the sample was observed to be decomposed. The undoped sample to be reduced was sealed in a quartz tube together with enough Cu<sub>2</sub>O powder and annealed at 1000 °C for 24 hours. After reduction, we removed a damaged surface layer of the sample by polishing.

Measurements of the resistivity and shielding signal have showed that the reduced sample of  $x = 0.15$  superconducts below 21 K. However, the shielding portion was as small as 20%, which is supposedly due to inhomogeneity of Ce content or immoderate reduction.

### B. Optical measurements

The optical spectrum was measured on the surface of the postannealed sample polished with alumina powder. We used a Fourier-transform-type interferometer and a grating-type monochromator for the photon energy of 0.012–0.8 and 0.6–38 eV, respectively. For the measurement above 6 eV, we utilized synchrotron radiation as a light source at INS-SOR, Institute of Solid State Physics, University of Tokyo. The incident angle was less than 15°, regarded as a normal incident reflection within a relative experimental accuracy of reflectivity of  $\sim 5\%$ .

The optical conductivity spectrum was calculated from the measured reflectivity spectrum using the Kramers-Kronig relation. We assumed the constant and Hagen-Rubens-type reflectivity for  $< 0.012$  eV in semiconducting and metallic samples, respectively, and the  $\omega^{-4}$ -type extrapolation for the higher-energy reflectivity above 36 eV in all the spectra.

## III. SPECTRA OF OPTICAL REFLECTIVITY AND CONDUCTIVITY

### A. Overall features and anisotropy

We show in Fig. 1 reflectivity spectra in the range of 0.01–40 eV for the undoped ( $x = 0$ ) and doped

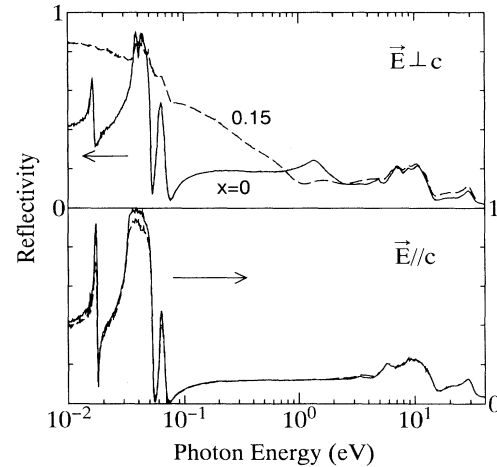


FIG. 1. Reflectivity spectra for the as-grown crystal of  $\text{Pr}_2\text{CuO}_4$  (solid lines) and  $\text{Pr}_{2-x}\text{Ce}_x\text{CuO}_{4-\delta}$  ( $x = 0.15$ ; broken lines) with light polarizations perpendicular (upper side) and parallel (lower side) to the  $c$  axis.

( $x = 0.15$ ) crystals (as grown) of  $\text{Pr}_{2-x}\text{Ce}_x\text{CuO}_{4-\delta}$  with light polarizations perpendicular (in plane) and parallel (out of plane) to the  $c$  axis. At a glance, one may notice that Ce substitution causes an appreciable change for the  $E \perp c$  spectra below 6 eV but very little change for the  $E \parallel c$  spectra in the whole energy region. Below 0.1 eV, four  $E_{2u}$  and three  $A_{2u}$  optical phonon modes show up in the  $E \perp c$  and  $E \parallel c$  spectra, respectively, which are expected from the  $D_{4h}$  symmetry.<sup>7</sup> Among them, the highest-lying mode at  $500 \text{ cm}^{-1}$  in the  $E \perp c$  spectra corresponds to in-plane Cu-O stretching vibrations. In the in-plane polarized spectra, the Ce-doping ( $x = 0.15$ ) considerably reduces the phonon structures due to the overlapping plasmlike high reflectance response, though they are still discernible.

Below 6 eV, where the Cu-O-related electronic transitions are involved, two in-plane polarized peaks are observed at 1.5 and 5.0 eV in the  $x = 0$  as-grown crystal. These are ascribed to the in-plane Cu-O related transitions: charge-transfer-type transitions from O  $2p$  to Cu  $3d_{x^2-y^2}$  and to Cu  $4s$ , respectively (*vide infra*). These in-plane interband transitions are extremely blurred or diminished upon Ce doping and instead a high reflectance band comes out accompanying an apparent plasma edge around 1.0 eV. Contrary to this, the out-of-plane ( $E \perp c$ ) spectra show a rather structureless feature in the range from 0.1 to 3 eV. Furthermore, no plasmlike response appears on Ce-doping at least above 0.01 eV and therefore no screening effect acts on the phonon spectra. If we could attribute such a large optical anisotropy of the plasmlike response observed in the  $x = 0.15$  crystal to anisotropy of optical carrier mass, the ratio  $m_c^*/m_{ab}^*$  would exceed  $10^3$ . The present spectroscopic result is in accord with the large anisotropy of dc conductivity, which amounts to as large as  $10^4$  in the as-grown  $x = 0.15$  crystal at room temperature.<sup>8</sup>

Let us briefly survey features of the higher-lying transi-

tions above 6 eV. Spectral profiles of those transitions are affected little by the carrier-doping procedure, implying that the change of electronic structures caused by carrier doping are restricted to the lower-lying electronic states inherent in the Cu 3d and O 2p related electronic states in the  $\text{CuO}_2$  sheets. The structures at 7–12 eV show some polarization-dependent features and may be mostly ascribed to the interband transitions from the O 2p valence bands to Pr 5d/4f conduction bands. Above 20 eV, the spectra show less anisotropy, which can be assigned to the intra-atomic electronic excitation such as Pr 5p-5d transitions.

### B. Change of spectra with compositions

We show in Fig. 2 in-plane polarized ( $E \perp c$ ) reflectivity spectra of  $\text{Pr}_{2-x}\text{Ce}_x\text{CuO}_{4-\delta}$  crystals with various Ce concentrations. Solid and dashed lines in the figure represent the spectra for the as-grown and reduced samples, respectively. (For details of the reducing procedure for each sample, see the descriptions in Sec. II B.) Systematic change of the spectra can be seen mostly below 6 eV where the optical transitions are relevant to O 2p and Cu 3d/4s states apart from optical phonons: with Ce doping a high reflectance band associated with an apparent plasma edge around 1 eV is standing out while diminishing the phonon peaks below 0.1 eV. In accord with this, the peak at 1.5 eV due to the charge-transfer gap excitation fades away.

To see the doping-induced changes more quantitatively, we show in Fig. 3 in-plane polarized spectra of optical conductivity  $\sigma(\omega)$  below 6 eV in the as-grown and reduced crystals of  $\text{Pr}_{2-x}\text{Ce}_x\text{CuO}_{4-\delta}$ . The  $\sigma(\omega)$  spectra were obtained by the aforementioned procedure of the Kramers-Kronig analysis of the corresponding reflectivity data shown in Fig. 2. As argued in Fig. 1, the two distinct peaks are observed at 1.5 and 5.0 eV in the spectra for the as-grown  $x=0$  (most insulating) crystal.

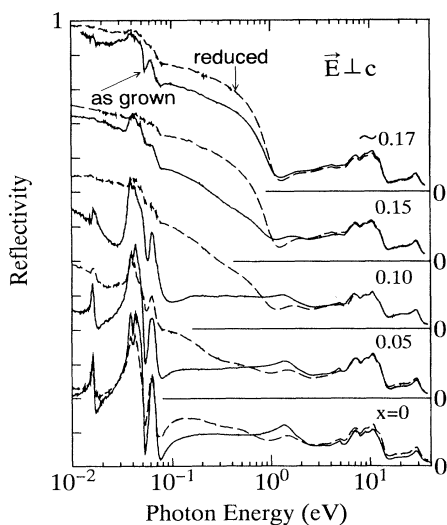


FIG. 2. In-plane polarized ( $E \perp c$ ) reflectivity spectra of as-grown (solid lines) and reduced (broken lines)  $\text{Pr}_{2-x}\text{Ce}_x\text{CuO}_{4-\delta}$  with various Ce concentrations.

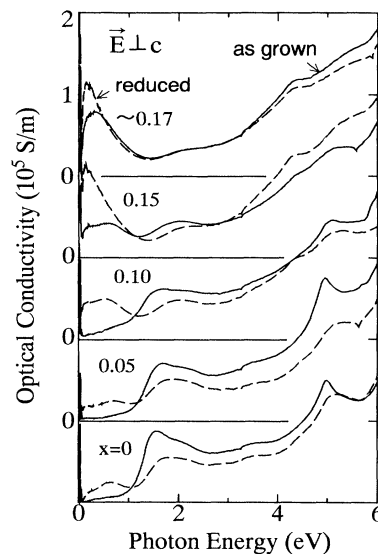


FIG. 3. In-plane polarized ( $E \perp c$ ) optical conductivity spectra of as-grown (solid lines) and reduced (broken lines)  $\text{Pr}_{2-x}\text{Ce}_x\text{CuO}_{4-\delta}$ .

We have assigned these transitions to the charge-transfer (CT)-type excitations from the O 2p like states to the Cu  $3d_{x^2-y^2}$  like states (upper Hubbard band) and to the Cu 4s like states, respectively.

Concerning the 1.5-eV transition, the assignment of the CT gap transition seems to be well established. A systematic variation of the CT gap energies in various layered cuprate compounds has been experimentally investigated,<sup>9</sup> which have been explained quantitatively<sup>10</sup> for the parent compounds of the high- $T_c$  cuprates. The 5.0-eV excitation is also completely polarized along the  $\text{CuO}_2$  sheet (see Fig. 1) and obviously related to electronic states in the  $\text{CuO}_2$  sheets. There may be other possible assignments for this transition; for example, 3d-3d transitions between lower and upper Hubbard bands or higher-lying 3d-2p CT transitions. As argued in our previous publication,<sup>11</sup> the observed 5.0-eV peak is too intense to be assigned to the d-d (Mott-Hubbard gap) transition. Another possible assignment that the 1.5 and 5.0-eV peaks are the transitions from the geminate O 2p states of the bonding (Zhang-Rice singlet) and nonbonding natures to the upper Hubbard (Cu 3d like) band was hinted in cluster calculations for the optical conductivity by Tohyama and Maekawa.<sup>12</sup> The assignment for the 5-eV band adopted here, that is the interband transition from O 2p to Cu 4s, is based on the consideration of the fairly high excitation energy and its material-dependent variation as well as a characteristic change of its spectral structure upon carrier doping (*vide infra*).

Next, let us overview the doping-induced changes in spectra below 6 eV. (Detailed analysis and discussion are presented in the next section.) The both conductivity peaks at 1.5 and 5.0 eV are blurred and decreased in intensity with Ce doping or by the reducing procedure, yet still clearly observed up to  $x=0.15$  for the as-grown crystals and to  $x=0.10$  for the reduced crystals. In ac-

cord with this change, a midinfrared absorption band appears below the CT gap region, as typically seen for the as grown  $x = 0.15$  sample and the reduced samples with  $x \leq 0.10$ . It is to be noted that in the higher-energy region there appears another conductivity peak around 4 eV in Ce doped ( $x \geq 0.15$ ) and reduced ( $x \geq 0.10$ ) samples while diminishing the 5-eV peak.

### C. Change of spectra with reducing treatments

The reducing treatment of the  $\text{Pr}_{2-x}\text{Ce}_x\text{CuO}_{4-\delta}$  compound also causes appreciable changes in reflectivity spectra. Very similar to the case of increasing  $x$ , the reducing procedure produces or enhances the infrared high reflectivity band as well as diminishes the peak intensity around 1.5 eV. The effect is quite appreciable in contrast with hardly observable change in lattice structure during reducing procedure.

As far as a change in the optical spectra is concerned, the reducing procedure appears to be almost equivalent to increasing the Ce concentration approximately by 0.05 apart from the case of  $x = 0$ : Compare, for example, the spectra in the as grown  $x = 0.15$  and reduced  $x = 0.10$  crystals, which show a very similar profile to each other (Fig. 4). Concerning the  $x = 0$  crystal, a more pronounced reducing effect was observed perhaps due to a larger amount of reduced oxygen content. If we can consider that reduction of the oxygen content simply corresponds to addition of the electron-type carriers to the  $\text{CuO}_2$  sheets as in increasing the Ce concentration, the electron count based on the above comparison of the spectra implies the reduced oxygen content of 0.02–0.03. This is consistent with the amount of oxygen deficiencies which were reported by chemical analysis for the reduced  $T'$ -phase compounds.<sup>5</sup> Thus, one of the important reducing effects is no doubt to increase the concentration of electron-type carriers. Nevertheless, we cannot discard the possibility that the reducing procedure plays an additional active role to realize the electronic states responsible for high- $T_c$ . For example, oxygen vacancies intro-

duced into the  $\text{CuO}_2$  sheet may be effective, even if a very few, to destroy the long-range antiferromagnetic spin order which is seen for all the as-grown Ce-doped compounds at low temperatures.<sup>13,14</sup> However, such an effect would be difficult to be distinguished from the effect of increasing the carrier density by the optical spectroscopy, and should be investigated by other low-energy probes.

### IV. GROWTH OF IN-GAP STATES WITH CARRIER DOPING

To see a detailed change of the spectral weight in the infrared region and CT gap region, we show in Fig. 5  $\sigma(\omega)$  spectra below 3 eV with varying  $x$  in a magnified scale for the as-grown crystals and some of the reduced crystals. The doping- or reducing-induced midinfrared band (see, for example, the spectra for the reduced  $x = 0$  and as grown  $x = 0.15$  crystals) seems to be composed of two or more components, i.e., peaks around 0.2 and 0.8 eV. These features are essentially in accord with the midinfrared bands observed in the reduced  $\text{Nd}_2\text{CuO}_4$  crystal whose origins were discussed in detail by Thomas *et al.*<sup>15</sup> They assigned these bands ( $J$  and  $I$  bands in their notation) to impurity bands associated with oxygen vacancies: The lower-lying  $J$  band was attributed to the nearest-neighbor hopping process of the bound (excess) electron on the Cu site accompanying a frustrated spin arrangement left behind, while the  $I$  band to the ionization process of the bound electron.

These peak structures in the midinfrared region show up prominently in the reduced crystals with low Ce concentrations ( $x = 0$ – $0.10$ ), but are hardly discernible for the as-grown  $x = 0.10$  crystals with comparable carrier density. This may support the above assignment by Thomas *et al.* However, the spectral weight below the CT gap energy is carried not only by the peak structures of the  $J$  and  $I$  bands, but also by the underlying broad contributions. With further increasing the carrier concentration by the Ce doping and reducing treatments, the higher-lying midinfrared band ( $I$  band) appears to shift toward lower energy, forming a single peak band together with the originally lower-lying band ( $J$  band). It is not

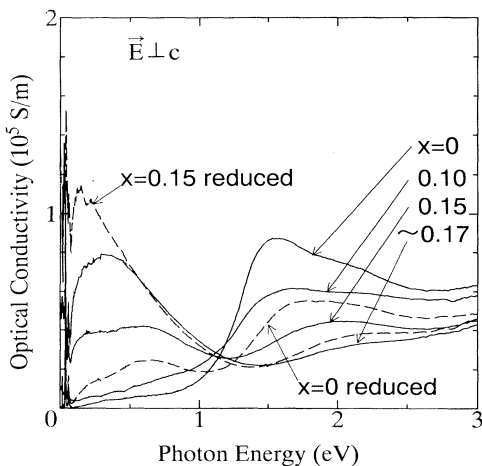


FIG. 4. Optical conductivity spectra of  $\text{Pr}_{2-x}\text{Ce}_x\text{CuO}_{4-\delta}$  with light polarization perpendicular to the  $c$  axis (in-plane).

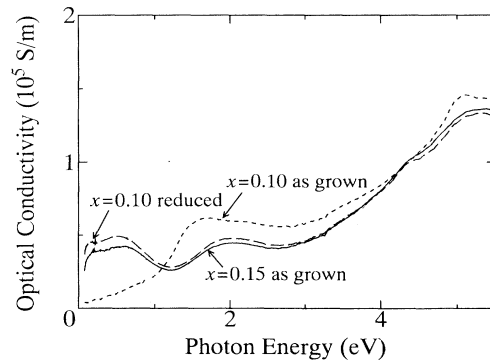


FIG. 5. Optical conductivity spectra of the as-grown  $\text{Pr}_{1.85}\text{Ce}_{0.15}\text{CuO}_4$  (solid line) and the reduced and as-grown  $\text{Pr}_{1.90}\text{Ce}_{0.10}\text{CuO}_{4-\delta}$  (broken and dotted lines, respectively) with the in-plane light polarization.

easy to specify conclusively the origin of the midinfrared absorption either to the aforementioned impurity band or to other intrinsic many-body effects (e.g., doping-induced Zhang-Rice singlet-like states<sup>16</sup>).

As a probe for the nature of the doping-induced states within the CT gap, a spectral change of the interband transition observed around 5 eV with doping is quite informative. We show in Fig. 6 the doping- and reducing-induced changes of the  $\sigma(\omega)$  spectra for the 5 eV transition in a magnified scale. It is clearly seen in the figure that the spectral weight around 5.0 eV is gradually reduced with doping and that a new shoulder around 4.2 eV grows in accord. The two structures appear to coexist in the intermediately carrier-doped region, e.g., in the as-grown  $x=0.15$  crystal. We have assigned the 5-eV peak to the transition from the filled O 2p like states to the unoccupied Cu 4s band. Then, the doping-induced spectral change is likely attributed to a change of the O 2p like state (initial state) rather than the Cu 4s like state (final state), since the O 2p states are strongly coupled with the Cu 3d states, where strong correlation effect must be considered and should be sensitive to carrier doping. Gradual transfer of the spectral weight from the 5.0-eV peak to the 4.2-eV shoulder indicates that the Ce substitutions and reducing procedures induce the filled states (i.e., in-gap states) within the CT gap as an initial state for the 4.2-eV transitions. If the Cu 4s band is little affected by carrier doping in  $\text{Pr}_{2-x}\text{Ce}_x\text{CuO}_{4-\delta}$ , the spectral change in peaks around 5 eV can be viewed as a change of density of states of the filled bands near below the Fermi level. A schematic drawing for the one-particle density of states near the Fermi level is presented in Fig. 7. The original 5.0 eV and doping-induced 4.2-eV peaks correspond to the transitions from the original topmost valence (O 2p) band and the in-gap states near below  $E_F$ , respectively, as indicated by arrows in Fig. 7.

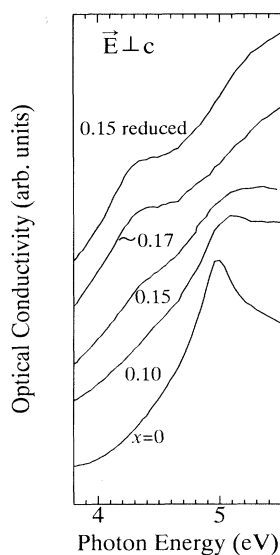


FIG. 6. Optical conductivity spectra of the  $\text{Pr}_{2-x}\text{Ce}_x\text{CuO}_{4-\delta}$  with light polarization perpendicular to the  $c$  axis (in-plane). The baseline for each spectrum is arbitrarily shifted.

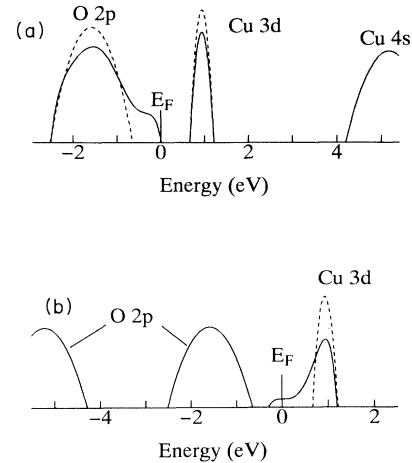


FIG. 7. Schematic drawing for the expected one-particle density of states near the Fermi level in the undoped (broken line) and lightly doped (solid line)  $\text{Pr}_{2-x}\text{Ce}_x\text{CuO}_{4-\delta}$ , when (a) one would assign the 5-eV transition to the O 2p-Cu 4s excitation, or (b) one would assign it to the O 2p-Cu 3d excitation.

In this view, the energy separation (ca. 0.8 eV) between the two peaks (or more correctly between the two absorption edges) must correspond to the energy distance between  $E_F$  and the upper edge of the O 2p band. The value is in agreement with the one (0.7 eV) estimated by the photoemission study on the related compound  $\text{Nd}_{2-x}\text{Ce}_x\text{CuO}_{4-\delta}$ .<sup>17</sup>

In the cases of electron doping and hole doping in cuprate systems<sup>17</sup> and perhaps also in the other Mott-Hubbard insulators, the doping-induced in-gap states are likely to be formed mainly below and above the Fermi level, respectively, as far as the compound remains insulating or barely metallic. One of the consequence of such a feature is a different behavior of the electron energy loss (EEL) and x-ray absorption spectra for the O 1s core level in hole-doped systems  $\text{La}_{2-x}\text{Sr}_x\text{CuO}_4$  (Ref. 18) and electron-doped systems  $\text{Nd}_{2-x}\text{Ce}_x\text{CuO}_{4-\delta}$  or  $\text{Pr}_{2-x}\text{Ce}_x\text{CuO}_{4-\delta}$  (Ref. 19). In the former case, the EEL and x-ray absorption spectroscopy has revealed the *unoccupied* doping-induced states (in-gap or gap-filling states) below the lower edge of the unoccupied Cu 3d states (upper Hubbard band),<sup>18</sup> whereas in the electron-doped systems no counterpart of the unoccupied in-gap states.<sup>19</sup> On the basis of these observations, Alexander *et al.*<sup>19</sup> have concluded that the Fermi level should be stuck to the bottom of the upper Hubbard band in the electron-doped systems. In contradiction, photoemission studies have shown that the Fermi level is pinned against electron doping within the original CT gap (at ca. 0.7 eV above the topmost valence states in the parent insulator).<sup>20</sup> This optical study can give a possible explanation for the apparent discrepancies reported by these high-energy spectroscopies. In short, the in-gap states in  $\text{Pr}_{2-x}\text{Ce}_x\text{CuO}_{4-\delta}$  and related compounds can be seen only as the initial states as in the optical and photoemission spectroscopies but hardly as the final states, since

most of the in-gap states in the electron-doped cuprates are formed below the Fermi level unlike the case of the hole-doped cuprate compounds. The EEL and x-ray absorption spectroscopies using the core level (e.g., O 1s) states as an initial state can only probe unoccupied final states. This may be why the EEL spectroscopy cannot detect the in-gap states in the electron-doped cuprates but the optical and photoemission studies can.

The 5-eV transition can also be assigned to the excitation from the nonbonding O 2*p* band to the upper Hubbard 3*d* band. In this case, the doping-induced change of the spectrum should be ascribed to the change of the upper Hubbard band with the doping rather than the O 2*p* band. The one-particle density of states near the Fermi level is presented schematically in Fig. 7(b), based on this assignment of the 5.0-eV optical transition. Here, the final state of the optical transition is changed through the carrier doping, which must be detected by the x-ray absorption spectra and electron-energy-loss spectra. This assignment is not consistent with the reported results of the core spectra mentioned above.

On the basis of the above argument, the midinfrared absorption (Fig. 4) may be interpreted as the transitions between the in-gap states and Cu 3*d* (upper Hubbard) band. The original CT gap is ca. 1.5 eV and the energy separation between the occupied in-gap states and unoccupied upper Hubbard band edge should be ca. 0.7 eV, which approximately equals to the energy of the *I* band (main midinfrared absorption peak).

To estimate the spectral weight of the in-gap state-related transitions, we have plotted in Fig. 8 the value of effective number of electrons  $N_{\text{eff}}$  at 1.1 eV as a function of Ce concentration  $x$ , for both of the as-grown and reduced crystals of  $\text{Pr}_{2-x}\text{Ce}_x\text{CuO}_{4-\delta}$ . Here,  $N_{\text{eff}}(\omega)$  is defined by the relation,

$$N_{\text{eff}}(\omega) = \frac{2m_0 V_{\text{cell}}}{\pi e^2} \int_0^\omega d\omega' \epsilon_0 \epsilon_2(\omega') \omega',$$

where  $V_{\text{cell}}$  is the primitive unit cell size. The photon energy 1.1 eV corresponds to the isosbestic point in spectral changes shown in Fig. 4 and can be a convenient measure for an estimation of the contribution of the in-gap states. Behavior of the spectral weight transfer (Fig. 8) observed in the present study is much different from the earlier data by Cooper *et al.*:<sup>4</sup> The present result shows a slower increase of  $N_{\text{eff}}$  against  $x$  than the previous study<sup>4</sup> on the flux-grown crystals. The infrared spectral weight shows somewhat threshold like increase against  $x$ ; around  $x = 0.10$  for the as-grown crystals and around  $x = 0.05$  for the reduced crystals. These particular  $x$  values are approximately corresponding to the nonmetal-metal boundaries at room temperature in the as-grown and reduced crystals of  $\text{Pr}_{2-x}\text{Ce}_x\text{CuO}_{4-\delta}$ .

The observed spectral weight transfer in the low-doped region is much slower than the case of the hole-doped  $\text{La}_{2-x}\text{Sr}_x\text{CuO}_4$  though the spectral weights at high doping ( $x \geq 0.15$ ) are comparable with each other. It is also concluded from the  $x$ - $N_{\text{eff}}$  plot (Fig. 8) that the reducing procedure seems to increase effectively the electron concentration by an equivalent amount of Ce concentration

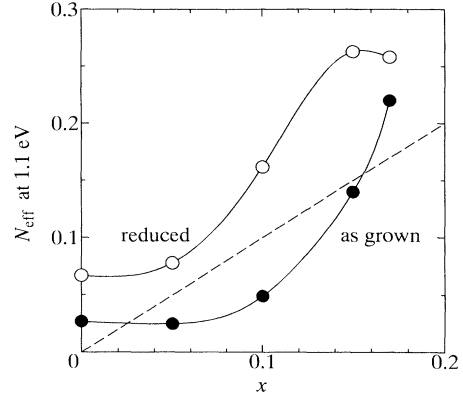


FIG. 8. Change of  $N_{\text{eff}}$  at 1.1 eV (the photon energy of the isosbestic point) with Ce concentration in  $\text{Pr}_{2-x}\text{Ce}_x\text{CuO}_{4-\delta}$ . A broken line represents the anticipated value in the case of the simple electron doping picture assuming that the doped electron has the effective mass of the bare electron.

( $\sim 0.05$ – $0.08$ ). The infrared spectral weight represents the  $n/m^*$  value which is measured with a relatively high-energy scale. A broken line in the figure represents the anticipated spectral weight transfer in the case that each Ce ion donates one mobile carrier with effective mass of  $m_e$  (the mass of bare electron). The observed behavior of  $N_{\text{eff}}$  at  $\omega = 1.1$  eV implies a crossover behavior of the effective carrier density (or the carrier effective mass) from low to high (or from heavy to light) with increasing  $x$ .

## V. CONCLUDING REMARKS

We have investigated changes of the optical conductivity spectra in the as-grown and reduced single crystals of  $\text{Pr}_{2-x}\text{Ce}_x\text{CuO}_{4-\delta}$ . With use of the fairly large single crystals grown by the traveling solvent floating-zone method, we could investigate the spectroscopic anisotropy, which would be difficult with use of conventional flux-grown crystals. With Ce doping or reducing oxygen content, the in-gap states are observed to grow in the original CT gap region mostly below the Fermi level. The growth behavior of the in-gap states in  $\text{Pr}_{2-x}\text{Ce}_x\text{CuO}_{4-\delta}$  is different from the case of hole-doped  $\text{La}_{2-x}\text{Sr}_x\text{CuO}_4$  system: The growth rate of the in-gap spectral weight in the low-doped region ( $x \leq 0.1$ ) is much lower than in  $\text{La}_{2-x}\text{Sr}_x\text{CuO}_4$ , indicating a heavier effective mass of the doped carriers. However, there seems to be a steep change of the electron states with carrier doping, as seen in the threshold, such as an increase in the infrared spectral weight.

## ACKNOWLEDGMENTS

We are grateful to A. Fujimori for helpful discussions. This work was supported by a Grant-in-Aid for Scientific Research from the Ministry of Education, Science, Culture of Japan.

- <sup>1</sup>For example, A. Fujimori, E. Takayama-Muromachi, Y. Uchida, and B. Okai, *Phys. Rev. B* **35**, 8814 (1987).
- <sup>2</sup>S. Uchida, T. Ido, H. Takagi, T. Arima, Y. Tokura, and S. Tajima, *Phys. Rev. B* **43**, 7942 (1991).
- <sup>3</sup>Z. Schlesinger, R. T. Collins, F. Holtzberg, C. Field, U. Welp, Y. Fang, and J. Z. Liu, *Phys. Rev. Lett.* **65**, 801 (1990).
- <sup>4</sup>S. L. Cooper, G. A. Thomas, J. Orenstein, D. H. Rapkine, A. J. Mills, S.-W. Cheong, A. S. Cooper, and Z. Fisk, *Phys. Rev. B* **41**, 11 605 (1990); Y. Tokura, T. Arima, S. Koshihara, T. Ido, S. Ishibashi, H. Takagi, and S. Uchida, in *Advances in Superconductivity II*, edited by T. Ishiguro and K. Kajimura (Springer-Verlag, Tokyo, 1990); E. V. Abel', V. S. Bagaev, D. N. Basov, O. V. Dolgov, A. F. Plotnikov, A. G. Poiarkov, and W. Sadovsky, *Solid State Commun.* **79**, 931 (1991).
- <sup>5</sup>F. Izumi, Y. Matui, H. Takagi, S. Uchida, Y. Tokura, and H. Asano, *Physica C* **158**, 433 (1989).
- <sup>6</sup>K. Oka and H. Unoki, in *Proceedings of the Second International Symposium on Superconductivity (ISS '89)*, edited by T. Ishiguro and K. Kajimura (Springer-Verlag, Tokyo, 1990).
- <sup>7</sup>S. Tajima, T. Ido, S. Ishibashi, T. Ito, E. Eisaki, T. Mizuo, T. Arima, H. Takagi, and S. Uchida, *Phys. Rev. B* **43**, 10 496 (1991).
- <sup>8</sup>T. Ito, H. Takagi, S. Ishibashi, T. Ido, and S. Uchida, *Nature (London)* **350**, 596 (1991).
- <sup>9</sup>Y. Tokura, S. Koshihara, T. Arima, H. Takagi, S. Ishibashi, T. Ido, and S. Uchida, *Phys. Rev. B* **41**, 11 657 (1990).
- <sup>10</sup>Y. Ohta, T. Tohyama, and S. Maekawa, *Phys. Rev. Lett.* **66**, 1228 (1991).
- <sup>11</sup>S. L. Cooper, G. A. Thomas, A. J. Millis, P. E. Sulewski, J. Orenstein, D. H. Rapkine, S.-W. Cheong, and P. L. Trevor, *Phys. Rev. B* **42**, 10 785 (1990); T. Arima, K. Kikuchi, M. Kasuya, S. Koshihara, Y. Tokura, T. Ido, and S. Uchida, *Phys. Rev. B* **44**, 917 (1991).
- <sup>12</sup>T. Tohyama and S. Maekawa, *J. Phys. Soc. Jpn.* **60**, 53 (1991).
- <sup>13</sup>G. M. Luke, B. J. Sternlieb, Y. J. Uemura, J. H. Brewer, R. Kadno, R. F. Kiefl, S. R. Kreitzman, T. M. Riseman, J. Gopalakrishnan, A. W. Sleight, M. A. Subramanian, S. Uchida, H. Takagi, and Y. Tokura, *Nature (London)* **338**, 49 (1989).
- <sup>14</sup>S. Kambe, H. Yasuoka, H. Takagi, S. Uchida, and Y. Tokura, *J. Phys. Soc. Jpn.* **60**, 400 (1991).
- <sup>15</sup>G. A. Thomas, D. H. Rapkine, S. L. Cooper, S.-W. Cheong, A. S. Cooper, L. F. Schneemeyer, and J. V. Waszczak, *Phys. Rev. B* **45**, 2474 (1992).
- <sup>16</sup>F. C. Zhang and T. M. Rice, *Phys. Rev. B* **37**, 3759 (1988).
- <sup>17</sup>H. Namatame, A. Fujimori, Y. Tokura, M. Nakamura, K. Yamaguchi, A. Misu, H. Matsubara, S. Suga, H. Eisaki, T. Ito, H. Takagi, and S. Uchida, *Phys. Rev. B* **41**, 7205 (1991).
- <sup>18</sup>C. T. Chen, F. Sette, Y. Ma, M. S. Hybertsen, E. B. Stechel, W. M. C. Foulkes, M. Schluter, S.-W. Cheong, A. S. Cooper, L. W. Rupp, Jr., B. Batlogg, Y. L. Soo, Z. H. Ming, A. Krol, and Y. H. Kao, *Phys. Rev. Lett.* **66**, 104 (1991).
- <sup>19</sup>M. Alexander, H. Romberg, N. Nücker, P. Adelman, J. Fink, J. T. Markert, M. P. Maple, S. Uchida, H. Takagi, Y. Tokura, A. C. W. P. James, and D. W. Murphy, *Phys. Rev. B* **43**, 333 (1991).
- <sup>20</sup>J. W. Allen, C. G. Olson, M. B. Maple, J.-S. Kang, L. Z. Liu, J.-H. Park, R. O. Anderson, W. P. Ellis, J. T. Markert, Y. Dalichaouch, and R. Liu, *Phys. Rev. Lett.* **64**, 595 (1990).